Journal of Applied Polymer Science

Dielectric Properties of Ag@C/PVDF Composites

Xiwen Kuang, Zhe Liu, Hong Zhu
State Key Laboratory of Chemical Resource Engineering, Institute of Modern Catalysis, Department of Organic Chemistry, School of Science, Beijing University of Chemical Technology, Beijing 100029, China
Correspondence to: H. Zhu (E-mail: zhuho128@126.com)

ABSTRACT: The core–shell Ag@C nanoparticles were prepared by hydrothermal method. The silver cores with diameters from 100 to 120 nm are each covered with a carbon shell about 60–80-nm thick. Ag@C/poly(vinylidene fluoride) (PVDF) composites were prepared by the solution cast method. Transmission electron microscopy showed that the Ag@C core–shell nanoparticles were dispersed homogenously in the PVDF matrix with little agglomeration. The crystallization behavior and dielectric properties of the Ag@C/PVDF composites as a function of frequency and temperature were studied. The differential scanning calorimeter measurements showed that the crystallinity of the Ag@C/PVDF composites decreased with the increasing content of the Ag@C nanoparticles. The dielectric tests showed that the permittivity of the Ag@C/PVDF composites increased obviously over that of the pure PVDF with increasing content of Ag@C particles because of the enhanced interfacial polarization. The tan δ of the composites remained at a low level (~0.08 at 1000 Hz). Furthermore, the permittivity and the tan δ of the composites increased with increasing temperature.
 J. Appl. Polym. Sci. 129: 3411–3416, 2013

KEYWORDS: core–shell; polymer composites; dielectrics; XRD

Received 29 October 2012; accepted 21 January 2013; published online 27 February 2013
DOI: 10.1002/app.39049

INTRODUCTION

Polymer-based composites with high permittivity (k) and low dielectric loss tangent (tan δ) have attracted much attentions because of their wide applications in capacitors, actuators, and sensors.[1–3] Traditional polymers are light-weight, flexible, and easily integrated. However, most polymers show a relatively low permittivity in the range of 2–5, which limited their commercial applications.[4] Much work has been focused on raising the k of polymer-based composites.[5] One effective method is to combine high-k ceramics with polymers to form organic-ceramic composites.[6–9] High loadings of ceramic fillers in the polymer matrix can increase the k of the composites, but dramatically decrease the compatibility and the flexibility of the composites. Another method is to introduce conductive fillers (e.g., Ag, Zn, and Ni) into the polymer matrix to form percolative composites.[10–12] The k of such composites is at least two orders of magnitude higher than that of the polymer matrix. However, the tan δ of these composites increases rapidly with increasing amount of conductive particles. In order to reduce tan δ, interlayers between the conductive fillers were used to prevent the fillers from directly connecting with each other. Therefore, core–shell materials with a metal as the core and an insulated material as the shell are expected to be ideal fillers for the polymer-based composites. Dang et al.[13] used Ag@TiO_2 core–shell nanoparticles as the filler in Ag@TiO_2/poly(vinylidene fluoride) (PVDF) composites and found that the permittivity of Ag@TiO_2/PVDF (50 wt %) composites was about 32 at 100 Hz. Nan and coworkers used Ag@C core–shell nanoparticles as the filler in Ag@C/epoxy composites and found that the dielectric constant of such composites is extremely high and the loss tangent is rather low.[14,15]

Poly (vinylidene fluoride) (PVDF) has been widely studied for many years because of its good mechanical, ferroelectric and piezoelectric properties.[16,17] It is a semicrystalline polymer with five kinds of phases in dependence of crystallization conditions. The most studied phases are the nonpolar α-phase with trans-gauche conformation, polar β-phase with all-trans conformation, and polar γ-phase with trans-trans-trans-gauche conformation.[18] The β-phase shows dielectric, piezoelectric, ferroelectric properties, and high permittivity; however, the most common phase in PVDF is the nonpolar α-phase.[19] Silver (Ag) is an important metallic material that has drawn much attention because of its high electrical and thermal conductivity and surface-enhanced Raman scattering.[20,21]

In this study, Ag@C core–shell nanoparticles were prepared by a hydrothermal method and the properties of the as-prepared Ag@C nanoparticles were characterized. Composites of Ag@C/

PVDF with different contents of Ag@C nanoparticles were prepared by the solution cast method. Transmission electron microscopy (TEM), X-ray diffraction (XRD), differential scanning calorimeter (DSC), and dielectric testing were used to characterize the properties of the composites. Besides, the effect of Ag@C nanoparticles on the dielectric properties of Ag@C/PVDF composites as a function of frequency and temperature was studied.

EXPERIMENTAL

Materials

Cetyltrimethylammonium bromide (CTAB) was bought from Tianjin Guangfu Fine Chemical Research Institute (China). Silver nitrate ($AgNO_3$) was purchased from Beijing Chemical Works (China). Ascorbic acid and dimethyl formamide (DMF) were bought from Sinopharm Chemical Reagent (China). Polyvinylidene fluoride (PVDF) was purchased from Solvay Advanced Polymers (Belgium).

Sample Preparations

Ag@C core–shell nanoparticles were prepared by a hydrothermal method.[22] 10 mL of 0.1*M* $AgNO_3$ was dissolved in 30 mL of de-ionized water, and then 0.1093 g of CTAB was put into the solution. After having been stirred for 10 min, 0.3523 g of ascorbic acid was added into the above solution. The resulting solution was stirred for another 10 min and then transferred to a 100-mL Teflon-lined autoclave. The hydrothermal synthesis was performed at 160°C for 24 h. After the reaction, the autoclave was allowed to cool in air and the suspension was centrifuged at 9,000 revolutions per minute for 30 min. The resulting precipitates were washed with ethanol and water three times and then dried at 80°C for 4 h.

Ag@C/PVDF composite membranes were prepared by the solution cast method. Predetermined amounts of Ag@C nanoparticles and PVDF were ultrasonically dispersed in DMF for 2 h until they were well dispersed in the solution. Then the solution was stirred vigorously for 8 h at 60°C. Afterwards, the solution was poured into a tank, which was then put into an oven at 80°C for 10 h to evaporate the solvent. After cooling down to ambient temperature, the content of the tank was annealed at 120°C for 4 h. Membranes with an average thickness of 100–120 μm were formed.

Characterizations

TEM observations were performed to analyze the detailed structure of the Ag@C core-shell nanparticle and the dispersion of Ag@C nanoparticles in the PVDF matrix by using a Jeol JEM-2010 transmission electron microscope running at 200 kV.

The XRD patterns of the Ag@C core–shell nanoparticle and composite membranes were recorded by using a Bruker D8 advanced diffractometer at room temperature. The X-ray source was Ni-filtered Cu Ka radiation (voltage 40 kV and current 30 mA). The samples were scanned at a speed of 0.5°/min from 10° to 80°.

The thermal behavior and crystallinity of PVDF and its composites were measured with a TA Instruments Q200 DSC at the heating and cooling rates of 10°C/min from room temperature to 200°C under nitrogen atmosphere. The weight of each sample was 5 mg. The first heating and second cooling traces of the samples were recorded.

The Raman spectrums of PVDF and its composites were recorded by a Renishaw microscope consisting of a 514-nm laser that supplies a 10-mW excitation beam at room temperature.

The dielectric properties of the composites were measured with an Agilent 4294A Precision Impedance Analyzer (Agilent) in the frequency range 1000 Hz to 10 MHz at room temperature and in the temperature range 10–130°C at 1000 Hz. Silver electrodes were sputtered on both sides of the composite films (about 10–15 μm thick) for the electrical measurements.

RESULTS AND DISCUSSION

TEM was used to evaluate the morphology of the Ag@C core–shell nanoparticles. As shown in Figure 1(a), a typical core–shell structure can be observed. The diameters of the silver cores are in the range 100–120 nm, while the thickness of the carbon shell is about 60–80 nm. Besides, the Ag@C core–shell nanoparticles are well separated from each other and show no agglomeration. Energy-dispersive X-ray spectroscopy (EDS) was used to determine the composition of the Ag@C nanoparticles. The EDS results shown in Figure 1(b) confirm that each obtained Ag@C nanoparticle is composed of a silver core and a carbon shell. Figure 1(c) shows the XRD pattern of the as-prepared Ag@C nanoparticles. The peaks at 38.0°, 44.1°, 64.4°, and 77.3° are assigned to the 111, 200, 220, and 311 lattice planes, respectively. These plans are indexed to be cubic-phase Ag. The calculated lattice constant was $a = 4.076$ Å, which is consistent with the standard value (JCPDS Card No. 04-0783).[22,23] The absence of a diffraction peak for AgO in the XRD pattern indicates that the Ag cores exist mainly as Ag^0 in the core–shell nanoparticles. Figure 1(d) shows the Raman spectra of the as-prepared Ag@C core–shell nanoparticles and the Ag@C/PVDF (10 wt %) composite. Because of the surface-enhanced Raman spectrum effect, the signals of the matrix are almost overwhelmed by those of the carbon shells. Hence the characteristic peaks from mainly the shells can clearly be seen. In both spectra, the two major peaks positioned at 1375 and 1585 cm^{-1} exist, which are attributed to the in-plane vibration of disordered amorphous carbon and crystalline graphic carbon, respectively.[24,25] Thus, the existence of the carbon shell in the composites is confirmed.

XRD was used to investigate the evolution of structure for PVDF and its composites with Ag@C particles. Figure 2 shows the XRD patterns of PVDF and Ag@C/PVDF composites with different contents of Ag@C nanoparticles. In the XRD pattern of PVDF, the peaks at 18.5, 20.0, and 36.3 are assigned to the (0 2 0), (1 1 0), and (2 0 0) lattice planes respectively, analogous to the characteristic peaks of the α-phase PVDF.[26] In the XRD patterns of the composites with different Ag@C contents, the existence of both the characteristic peaks of cubic-phase Ag and the characteristic peaks of α-phase PVDF, indicate that the Ag@C nanoparticles exist in the polymer matrix. No obvious changes in the position of the diffraction peaks of PVDF in the composites have been found, indicating that the addition of Ag@C nanoparticles does not affect the structure of the PVDF matrix. Besides, with the increase of Ag@C content, the

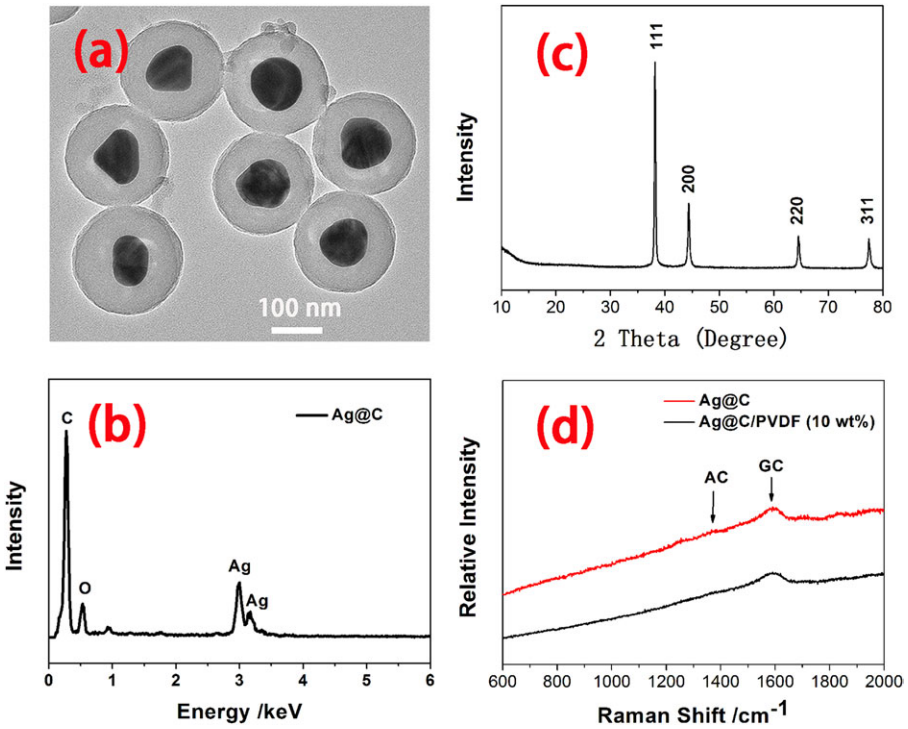

Figure 1. (a) TEM image of Ag@C, (b) EDS spectrum of Ag@C, (c) XRD pattern of Ag@C, and (d) Raman spectra of Ag@C and Ag@C/PVDF (10 wt %) composite. [Color figure can be viewed in the online issue, which is available at wileyonlinelibrary.com.]

intensity of the α-phase PVDF peaks decreases and the intensity of the cubic-phase Ag peaks become dominant because of high content of Ag@C nanoparticles in the polymer-based composites.

TEM was used to evaluate the dispersion of the Ag@C core–shell nanoparticles in the polymer matrix. Figure 3 shows the TEM photograph of the Ag@C/PVDF (10 wt %) composite. It can be seen that the Ag@C nanoparticles are dispersed homogenously in the polymer matrix and show little agglomeration. The good dispersion is attributed to the existence of the carbon shells, which provide good compatibility between the silver cores and the PVDF matrix. Besides, the solution cast method with vigorous stirring and ultrasonic treatment also contribute to the good dispersion. From the TEM photograph, we can also see that the addition of Ag@C nanoparticles does not affect the structure of the PVDF matrix, in accordance with the XRD results above.

The crystallization behavior of PVDF and Ag@C/PVDF composites with different content of Ag@C were studied by using differential scanning calorimetry at 10°C/min from 30 to 200°C. The DSC thermograms (the first heating and second cooling traces were recorded) of PVDF and Ag@C/PVDF composites are shown in Figure 4 and the corresponding parameters are summarized in Table I. In the first heating endotherm of PVDF, the peak around 164°C corresponds to the melting point (T_m) of

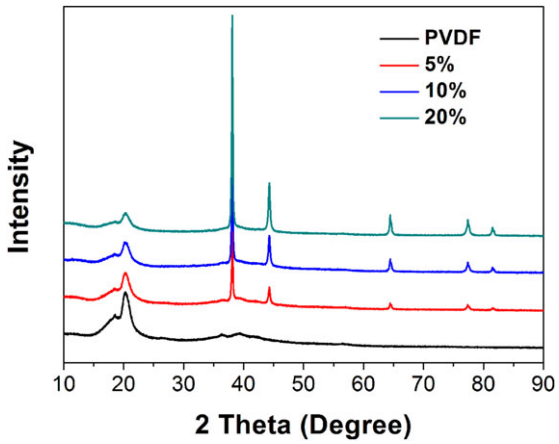

Figure 2. XRD patterns of PVDF and Ag@C/PVDF composites with different contents of Ag@C nanoparticles. [Color figure can be viewed in the online issue, which is available at wileyonlinelibrary.com.]

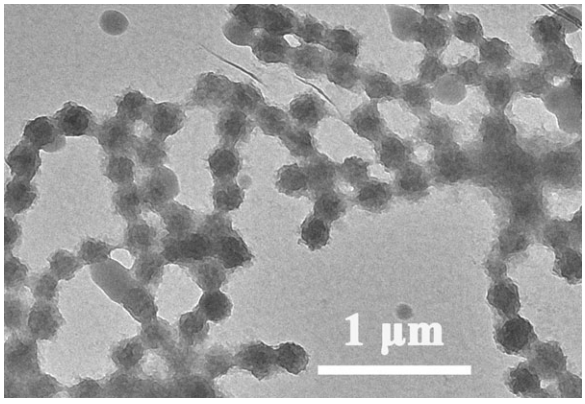

Figure 3. TEM photograph of Ag@C/PVDF (10 wt %).

Applied Polymer SCIENCE

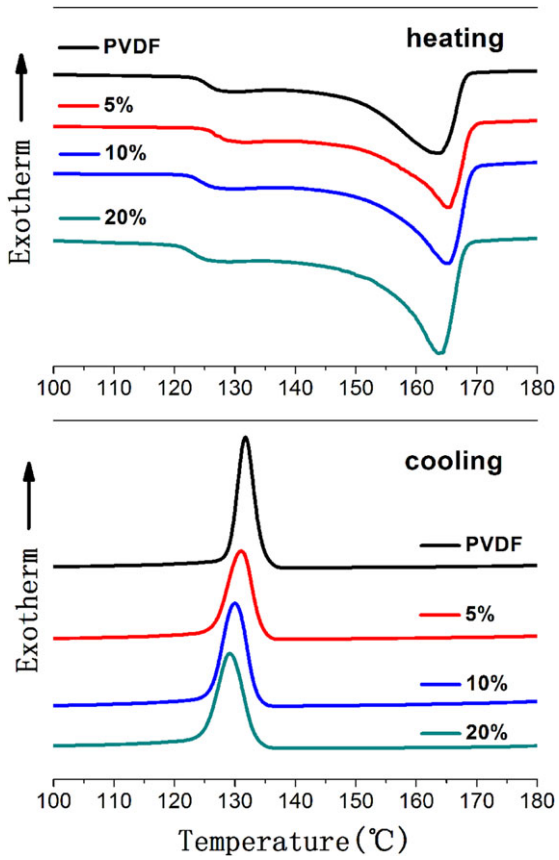

Figure 4. DSC thermograms of PVDF and PVDF/Ag@C composites with different content of Ag@C nanoparticles. [Color figure can be viewed in the online issue, which is available at wileyonlinelibrary.com.]

PVDF. In the Ag@C/PVDF composites, the positions of the melting peaks remain almost unchanged from that of the melting peak of PVDF, indicating that the Ag@C nanoparticles in the composites do not affect the melting behavior of PVDF. Besides, as the Ag@C content increases, the enthalpy of melting decreases obviously. The enthalpy for PVDF is about 19.19 J/g, while the values for Ag@C/PVDF composites are 18.45 J/g (5 wt %), 16.12 J/g (10 wt %), and 15.64 J/g (20 wt %) respectively. The decrease in enthalpy also indicates a decrease in the crystallinity of the composites. This result is in accordance with the results presented above. In the cooling cycle, the crystallization temperature (T_c) decreases with the increase of the Ag@C content. The decrease of T_c with Ag@C content indicate lower crystallinity of the composites than that of PVDF as a result of the Ag@C nanoparticles in the composites serving as anti-nucleating agents and hindering the crystallization of PVDF in the composites.

Table I. DSC Parameters of PVDF and Ag@C/PVDF Composites

Sample	ΔH_m (J/g)	T_m (°C)	T_c (°C)	X_c (%)
PVDF	19.19	163.85	131.71	18.28
5%	18.45	165.50	130.95	17.57
10%	16.12	165.31	130.04	15.35
20%	15.64	163.79	129.35	14.90

The DSC paramters ΔH_m, T_m, and T_c were summarized in Table I. The degree of crystallinity (X_c) of PVDF and Ag@C/PVDF composites can be calculated by using the following equation:

$$X_c(\%) = \frac{\Delta H_m}{\Delta H_0} \quad (1)$$

where ΔH_m is the enthalpy of melting of the sample (J/g), $\Delta H_0 = 105$ J/g is the enthalpy of fusion for 100% crystalline PVDF.[27] The calculated X_c results are also shown in Table I. The X_c for PVDF is 18.28%, and the values for the composites are 17.57% (5 wt %), 15.35% (10 wt %), and 14.90% (20 wt %), respectively. The decrease in X_c suggests decreases in crystallinity of PVDF in the composites. The Ag@C particles in the composites serve as anti-nucleation agents and hinder the crystallization of α-phase PVDF, thus reducing the crystallinity of the composites.

The dielectric permittivity (k) and dielectric loss tangent (tan δ) of PVDF and its composites with different contents of Ag@C nanoparticles as a function of frequency ranging from 1000 Hz to 10 MHz at room temperature are shown in Figure 5. As shown in Figure 5(a), the permittivities of PVDF and Ag@C/PVDF composites decrease with increasing frequency because of the decrease in dipolar contribution at high frequencies.[28,29] Besides, the permittivities of the Ag@C/PVDF composites

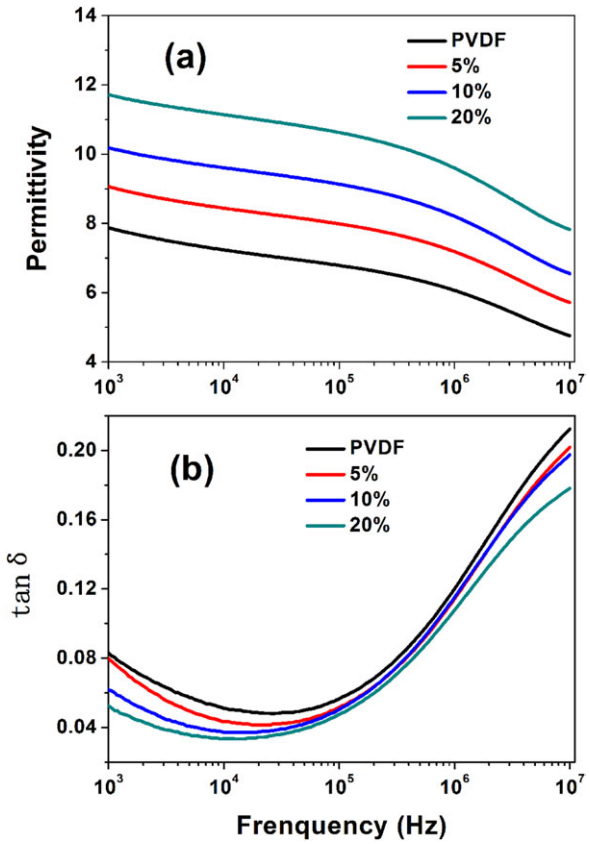

Figure 5. (a) Dielectric permittivity and (b) dielectric loss tangent (tan δ) of PVDF and its composites with different contents of Ag@C nanoparticles as a function of frequency at room temperature. [Color figure can be viewed in the online issue, which is available at wileyonlinelibrary.com.]

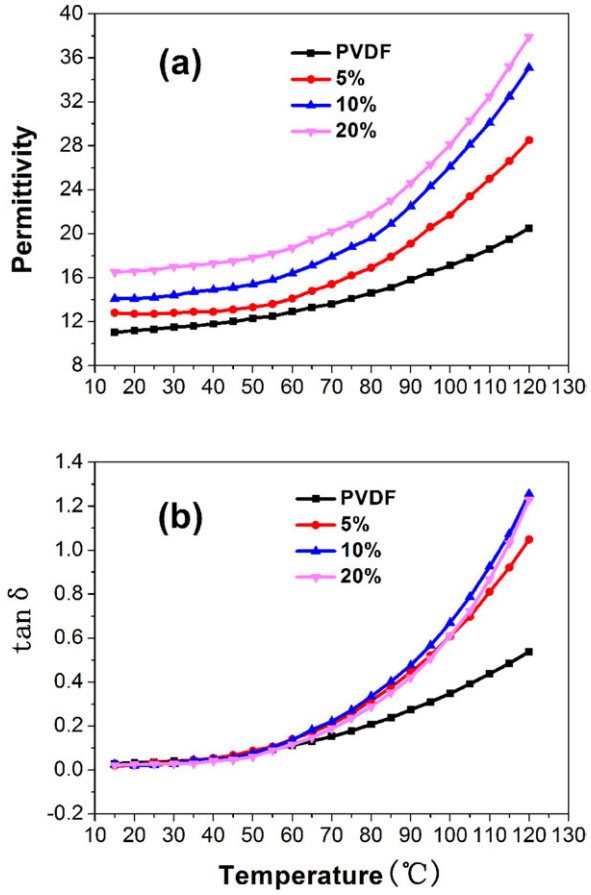

Figure 6. (a) Dielectric permittivity and (b) dielectric loss tangent (tan δ) of PVDF and its composites with different contents of Ag@C nanoparticles as a function of temperature at 1000 Hz. [Color figure can be viewed in the online issue, which is available at wileyonlinelibrary.com.]

increase with increasing content of Ag@C nanoparticles. For instance, Ag@C/PVDF with an Ag@C content of 20 wt % has a permittivity of 11.7 at 1000 Hz, which is much higher than the corresponding value of 7.8 for PVDF. The increase in permittivity is attributed to the enhanced interfacial polarization, which often occurs in dielectric composites of two or more components with different electrical properties. The interfacial polarization is associated with the entrapment of free charges generated in the cores at the interfaces between the cores and the matrix. As shown in Figure 5(b), the tan δ is very low at 1000 Hz for all the composites and shows little variation with the content of Ag@C nanostructured particles. The low tan δ can be ascribed to the carbon layer, which serves as an insulating interface to prevent the leakage of current caused by the direct contact of Ag particles. The carbon layer also produces good compatibility between the fillers and the polymer matrix.

Figure 6 shows the temperature dependence of the dielectric permittivity and dielectric loss tangent of PVDF and its composites with different contents of Ag@C nanoparticles at 1000 Hz. As shown in Figure 6(a), the permittivities of PVDF and its composites increase slowly below 60°C and then quickly above 60°C. In Figure 6(b), the tan δ of PVDF and its composites shows little variation below 60°C and then increases rapidly with temperature, suggesting that the temperature has a significant effect on the electrical polarization of PVDF and Ag@C/PVDF composites. An increase in temperature increases the molecular polarization of PVDF and the conductivity of the Ag nanoparticles in Ag@C, leading to the increase in conductivity, and hence permittivity and tan δ of the Ag@C/PVDF composites.

CONCLUSIONS

The Ag@C core–shell nanoparticles with a silver core 100 to 120 nm in diameter and a carbon shell 60 to 80 nm in thickness were prepared by a hydrothermal method. The Ag@C particles were homogenously dispersed in the PVDF matrix and had an effect on the crystallization behavior and dielectric properties of the Ag@C/PVDF composites. As the content of the Ag@C particles increased, the crystallinity of the composites decreased. The permittivity of the Ag@C/PVDF composites increased with increasing content of Ag@C particles because of the enhanced interfacial polarization. The tan δ of the composites remained at a low level even with increasing Ag@C content because of the carbon shells acting as interparticle barriers to prevent the direct contact of Ag particles. Furthermore, the permittivity and the tan δ of the composites increased with the increase of temperature.

ACKNOWLEDGMENTS

The authors gratefully acknowledge by National High Technology Research and Development Program of China (No. 2011AA11A273), National Defense Basic Scientific Research Program of China (No. A1420110023), National Natural Science Foundation of China (No. 20876013and 21176022), and International S&T Cooperation Program of China (No. 2009DFA63120).

REFERENCES

1. Zhang, Q. M.; Li, H.; Poh, M.; Xia, F.; Cheng, Z. Y.; Xu, H.; Huang, C. *Nature* **2002**, *419*, 284.
2. Kułek, J.; Szafraniak, I.; Hilczer, B.; Połomska, M. *J. Non-Cryst. Solids* **2007**, *353*, 4448.
3. Bauer, S. *J. Appl. Polym. Sci.* **1996**, *80*, 5531.
4. Chen, Q.; Wang, Y.; Zhou, X.; Zhang, Q. M.; Zhang, S. *Appl. Phys. Lett.* **2008**, *92*, 142909.
5. Dang, Z. M.; Yuan, J. K.; Zha, J. W.; Zhou, T.; Li, S. T.; Hu, G. H. *Prog. Mater. Sci.* **2012**, *57*, 660.
6. Arbatti, M.; Shan, X.; Cheng, Z. Y. *Adv. Mater.* **2007**, *19*, 1369.
7. Kobayashi, Y.; Tanase, T.; Tabata, T.; Miwa, T., Konno, M. *J. Eur. Ceram. Soc.* **2008**, *28*, 117.
8. Hu, Y. W.; Yu, S. H.; Sun, R.; Du, R. X. *Acta Mater.* **2011**, *59*, 5593.
9. Dang, Z. M.; Xu, H. P.; Wang, H. Y. *Appl. Phys. Lett.* **2007**, *90*, 012901.
10. Zhang, Y.; Wang, Y.; Deng, Y.; Li, M.; Bai, J. *Mater. Lett.* **2012**, *72*, 9.

11. Dang, Z. M.; Lin, Y. H.; Nan, C.W. *Adv. Mater.* **2003**, *15*, 1625.
12. Qi, L.; Lee, B. I., Chen, S.; Samuels, W. D.; Exarhos, G. J. *Adv. Mater.* **2005**, *17*, 1777.
13. Dang, Z. M.; You, S. S.; Zha, J. W.; Song, H. T.; Li, S. T. *Phys. Stat. Sol. A* **2010**, *207*,739.
14. Shen, Y.; Lin, Y. H.; Li, M.; Nan, C. W. *Adv. Mater.* **2007**, *19*, 1418.
15. Shen, Y.; Lin, Y. H.; Nan, C. W. *Adv. Funct. Mater.* **2007**, *17*, 2405.
16. Kawai, H. *Jpn. J. Appl. Phys.* **1969**, *8*, 975.
17. Lovinger, A. J. *Science* **1983**, *220*, 1115.
18. Davis, G. T.; McKinney, J. E.; Broadhurst, M. G.; Roth, S. C. *J. Appl. Polym. Sci.* **1978**, *49*, 4998.
19. Li, W.; Meng, Q.; Zheng, Y.; Zhang, Z.; Xia, W.; Xu, Z. *Appl. Phys. Lett.* **2010**, *96*, 192905.
20. Sun, Y.; Xia, Y. *Adv. Mater.* **2002**, *14*, 833.
21. Chen, L. M.; Liu, Y. N. *ACS Appl. Mater. Inter.* **2011**, *3*, 3091.
22. Fang, Z.; Tang, K.; Lei, S.; Li, T. *Nanotechnology* **2006**, *17*, 3008.
23. Sun, S. M.; Wang, W. Z.; Zhang, L.; Shang, M.; Wang, L. *Catal. Commun.* **2009**, *11*, 290.
24. Sun, X. M.; Li, Y. D. *Langmuir* **2005**, *21*, 6019.
25. Ilie, A.; Durkan, C.; Milne, W. I.; Welland, M. E. *Phys. Rev. B* **2002**, *66*, 045412.
26. Meng, Q.; Li, W.; Zheng, Y.; Zhang, Z. *J. Appl. Polym. Sci.* **2010**, *116*, 2674.
27. Tao, M. M.; Liu, F.; Xue, L. X. *Ultrason. Sonochem.* **2013**, *20*, 232.
28. Lu, Y.; Claude, J.; Norena-Franco, L. E.; Wang, Q. *J. Phys. Chem. B* **2008**, *112*, 10411.
29. Xia, W.; Xu, Z.; Wen, F.; Zhang, Z. *Ceram. Int.* **2012**, *38*, 1071.